

Demonstration of wavelength conversion at 40 Gb/s data rate in silicon waveguides

Ying-Hao Kuo, Haisheng Rong, Vanessa Sih, Shengbo Xu, and Mario Paniccia

Intel Corporation
2200 Mission College Blvd, SC12-326 Santa Clara, CA 95054
haisheng.rong@intel.com

Oded Cohen

Intel Corporation
S. B. I. Park Har Hotzvim, Jerusalem, 91031, Israel

Abstract: We report an efficient wavelength conversion via four-wave-mixing in reverse biased silicon-on-insulator p-i-n rib waveguides and demonstrate, for the first time, the conversion of a high-speed optical pseudo-random bit sequence data at 40 Gb/s. Results give a wavelength conversion efficiency of -8.6dB using a 8cm long waveguide with clear open eye on the wavelength converted signal. Conversion efficiency as functions of pump power and bias voltages has also been investigated. We show a slope efficiency close to 2 as predicted by theory.

©2006 Optical Society of America

OCIS codes: (190.4380) Nonlinear optics; Four-wave mixing; (203.7370) Waveguides; (190.2620) Frequency conversion; (230.4320) Nonlinear optical devices; (250.5300) Photonic integrated circuits; (060.4510) Optical communications

References and Links

1. S. J. B. Yoo, "Wavelength conversion technologies for WDM network applications," *J. Lightwave Technol.* **14**, 955-966 (1996).
2. B. Ramamurthy and B. Mukherjee, "Wavelength conversion in WDM networking," *IEEE J. Sel. Areas Commun.* **16**, 1061-1073 (1998).
3. T. Durhuus; B. Mikkelsen, C. Joergensen, S. L. Danielsen, and K. E. Stubkjaer, "All-optical wavelength conversion by semiconductor optical amplifiers," *J. Lightwave Technol.* **14**, 942-954 (1996).
4. D. Nesses, T. Kelly, and D. Marcenac, "All-optical wavelength conversion using SOA nonlinearities," *IEEE Commun. Mag.* **36**, 56-61 (1998).
5. D. Nesses; D. D. Marcenac, P. L. Mason, A. E. Kelly, S. Bouchoule, and E. Lach, "Simultaneous wavelength conversion of two 40 Gbit/s channels using four-wave mixing in a semiconductor optical amplifier," *Electron. Lett.* **34**, 107-108 (1998).
6. K. K. Chow, C. Shu, L. Chinlon, and A. Bjarklev, "Polarization-insensitive widely tunable wavelength converter based on four-wave mixing in a dispersion-flattened nonlinear photonic crystal fiber," *Photon. Technol. Lett.* **17**, 624-626 (2005).
7. J. H. Lee; T. Nagashima, T. Hasegawa, S. Ohara, N. Sugimoto, K. Kikuchi, "Four-wave-mixing-based wavelength conversion of 40-Gb/s nonreturn-to-zero signal using 40-cm bismuth oxide nonlinear optical fiber," *Photon. Technol. Lett.* **17**, 1474-1476 (2005).
8. L. Pavesi and D. J. Lockwood, *Silicon Photonics* (Springer-Verlag, New York, 2004).
9. G. T. Reed and A. P. Knights, *Silicon Photonics: An Introduction* (John Wiley, Chichester, UK, 2004).
10. L. Pavesi and G. Guillot, *Optical Interconnects - the silicon approach* (Springer-Verlag, Heidelberg, 2006).
11. A. Liu, H. Rong, M. Paniccia, O. Cohen, and D. Hak, "Net optical gain in a low loss silicon-on-insulator waveguide by stimulated Raman scattering," *Opt. Express* **12**, 4261-4268 (2004).
12. Q. Xu, V. R. Almeida, and M. Lipson, "Time-resolved study of Raman gain in highly confined silicon-on-insulator waveguides," *Opt. Express* **12**, 4437-4442 (2004).
13. T. K. Liang and H. K. Tsang, "Efficient Raman amplification in silicon-on-insulator waveguides," *Appl. Phys. Lett.* **85**, 3343-3345 (2004).
14. O. Boyraz and B. Jalali, "Demonstration of 11dB fiber-to-fiber gain in a silicon Raman amplifier," *IEICE Elect. Express* **1**, 429-434 (2004).
15. R. Jones, H. Rong, A. Liu, A. W. Fang, M. J. Paniccia, D. Hak, O. Cohen, "Net continuous wave optical gain in a low loss silicon-on-insulator waveguide by stimulated Raman scattering," *Opt. Express* **13**, 519-525 (2005).
16. O. Boyraz and B. Jalali, "Demonstration of a silicon Raman laser," *Opt. Express* **12**, 5269-5273 (2004).

17. H. Rong, A. Liu, R. Jones, O. Cohen, D. Hak, R. Nicolaescu, A. Fang, and M. Paniccia, "An all-silicon Raman laser," *Nature* **433**, 292-294 (2005).
18. H. Rong, R. Jones, A. Liu, O. Cohen, D. Hak, A. Fang, and M. Paniccia, "A continuous-wave Raman silicon laser," *Nature* **433**, 725-728, (2005).
19. H. Rong, Y.-H. Kuo, S. Xu, A. Liu, R. Jones, M. Paniccia, O. Cohen, and O. Raday, "Monolithic integrated Raman silicon laser," *Opt. Express* **14**, 6705-6712 (2006).
20. Q. Xu, V. R. Almeida, and M. Lipson, "Micrometer-scale all-optical wavelength converter on silicon," *Opt. Lett.* **30**, 2733-2735 (2005).
21. V. Raghunathan, R. Claps, D. Dimitropoulos, and B. Jalali, "Wavelength conversion in silicon using Raman induced four-wave mixing," *Appl. Phys. Lett.* **85**, 34-36 (2004).
22. R. L. Espinola, J. I. Dadap, R. M. Osgood, Jr., S. J. McNab, and Y. A. Vlasov, "C-band wavelength conversion in silicon photonic wire waveguides," *Opt. Express* **13**, 4341-4349 (2005).
23. H. Fukuda, K. Yamada, T. Shoji, M. Takahashi, T. Tsuchizawa, T. Watanabe, J. Takahashi, and S. Itabashi, "Four-wave mixing in silicon wire waveguides," *Opt. Express* **13**, 4629-4637 (2005).
24. T. Tsuchizawa, K. Yamada, H. Fukuda, T. Watanabe, Jun-ichi Takahashi; M. Takahashi, T. Shoji, E. Tamechika, S. Itabashi, H. Morita, "Microphotonic devices based on silicon microfabrication technology," *IEEE J. Sel. Topics. Quantum Electron.* **11**, 232 – 240 (2005).
25. H. Rong, Y.-H. Kuo, A. Liu, M. Paniccia, O. Cohen, "High efficiency wavelength conversion of 10 Gb/s data in silicon waveguides," *Opt. Express* **14**, 1182-1188 (2006).
26. K. Yamada, H. Fukuda, T. Tsuchizawa, T. Watanabe, T. Shoji, and S. Itabashi, "All-optical efficient wavelength conversion using silicon photonic wire waveguide," *IEEE Photon. Technol. Lett.* **18**, 1046-1048 (2006).
27. M. A. Foster¹, A. C. Turner, J. E. Sharping¹, B. S. Schmidt, M. Lipson, and A. L. Gaeta, "Broad-band optical parametric gain on a silicon photonic chip," *Nature* **441**, 960-963 (2006).
28. H. Rong, A. Liu, R. Nicolaescu, M. Paniccia, O. Cohen, and D. Hak, "Raman gain and nonlinear optical absorption measurements in a low-loss silicon waveguide," *Appl. Phys. Lett.* **85**, 2196-2198 (2004).
29. T. K. Liang and H. K. Tsang, "Role of free carriers from two-photon absorption in Raman amplification in silicon-on-insulator waveguides," *Appl. Phys. Lett.* **84**, 2745-2747 (2004).
30. R. Claps, V. Raghunathan, D. Dimitropoulos, and B. Jalali, "Influence of nonlinear absorption on Raman amplification in silicon waveguides," *Opt. Express* **12**, 2774-2780 (2004).
31. G. P. Agrawal, *Nonlinear Fiber Optics*, 2nd edition (Academic Press, New York, 1995).
32. Y.-H. Kuo, H. Rong, and M. Paniccia, "High bandwidth silicon ring resonator Raman amplifier," *IEEE 3rd International Conference on GroupIV Photonics, FB2, Ottawa, Sept. 2006.*
33. D. Dimitropoulos, V. Raghunathan, R. Claps, and B. Jalali, "Phase-matching and nonlinear optical processes in silicon waveguides," *Opt. Express* **12**, 149-160 (2004).

1. Introduction

A wavelength converter is one of the key components in multi-channel optical communication networks. In particular, all-optical wavelength converters offer the advantages of high speed, modulation format and bit rate transparency [1, 2]. Various all-optical wavelength converters based on nonlinear optical effects have been proposed using semiconductor optical amplifier (SOA) [3-5] or highly nonlinear fibers (HNLF) [6, 7]. However, the materials used in these devices tend to be expensive or bulky and incompatible with future silicon-based low-cost optoelectronics integration. Recently, silicon has been identified as a viable optical material and silicon photonics has emerged as a promising technology platform for low-cost solutions to optical communications and interconnects [8-10]. One of the important branches in silicon photonics is the application of various nonlinear optical effects in silicon to create active photonics devices. Due to high index contrast, light can be confined in silicon waveguides much more tightly than in glass fiber or silica based waveguides. The optical modal area in silicon waveguides can be more than 10^3 times smaller than in single mode fibers. Therefore, in silicon waveguides, the optical power density can be much higher and nonlinear effects are therefore greatly enhanced. Many of the concepts and applications already developed based on nonlinear optical effects in silica fibers can be adapted to silicon waveguides to produce compact, chip-scale, active photonics devices for various applications such as amplifiers[11-15], lasers[16-19], and wavelength converters[20-26]. All-optical wavelength conversion based on four-wave mixing (FWM) in silicon waveguides at data transfer rate up to 10Gb/s and conversion efficiency as high as -8.5 dB has been achieved [25, 26] which is compatible to HNLF based devices with similar pump power levels. Recently conversion efficiency up to 5.2dB has been reported on a silicon photonic chip using pico-second pulsed pump [27]. Although conversion at data rate of 40Gb/s or higher has been achieved in SOA or HNLF systems [5, 7], it has not been reported in silicon based devices. In this paper, we demonstrate

FWM based wavelength conversion in silicon waveguides with data rate of 40Gb/s. Our result shows that silicon-based wavelength converters are capable of high speed data transfer for next generation optical networking, such as OC-768.

2. Device description

The silicon rib waveguides are fabricated on the (100) surface of a silicon-on-insulator (SOI) substrate using standard photolithographic patterning and reactive ion etching techniques. The rib waveguide width is 1.5 μm , the rib height is 1.55 μm , and the etch depth is 0.7 μm . The waveguide is formed in double S-bend with total length of 8 cm (see Fig. 1). All bends have a bend radius of 400 μm . The straight sections of the waveguides are oriented along the [011] direction. To reduce the nonlinear optical loss due to the two photon absorption (TPA) induced free carrier absorption (FCA) [28-30], a p-i-n diode structure is fabricated by implanting boron and phosphorus in the slab on either side of the rib waveguide with a doping concentration of $\sim 1 \times 10^{20} \text{ cm}^{-3}$. The separation between the p and n type doped regions is 8 μm . By reverse biasing the diode, we can decrease the density of free carriers in the waveguide to reduce the nonlinear loss. [15] Aluminum films are deposited on the p and n doped regions to form ohmic contacts. The linear optical transmission loss of the waveguides is $0.4 \pm 0.1 \text{ dB/cm}$; measured using the Fabry-Perot resonance technique [9] prior to anti-reflection coating the silicon waveguide facets. The 0.1 dB/cm uncertainty in the linear optical loss includes the experimental error and waveguide-to-waveguide variations.

3. Experiments and results

A schematic of the experimental setup is shown in Fig. 1. The pump laser is a CW external cavity laser emitting around 1557.5 nm, which is amplified using an erbium doped fiber amplifier (EDFA) system to a output power of up to 1.26 W. The input signal is located at 1556.1nm and modulated by an external lithium niobate modulator. The pump and signal lasers are combined with a 100GHz add/drop (A/D) wavelength multiplexer centered at the pump wavelength. This narrow band filter also reduces the residual amplified spontaneous emission (ASE) from the EDFA. A lensed single-mode fiber is used to couple light into the waveguide. The coupling loss between the lensed fiber and the waveguide is measured to be 4 dB. The output beam of the waveguide is coupled into another lensed single-mode fiber. Another 100GHz A/D filter is used at the output to suppress the transmitted residual pump. The output beam is split into two paths. One portion ($\sim 10\%$) is fed into an optical spectrum analyzer (OSA) in order to analyze the spectrum of the output light. The remaining portion ($\sim 90\%$) is sent through a 200GHz A/D de-multiplexer which separates the converted signal from the input signal and the pump residue. An EDFA is used after the A/D filter to amplify the signal. An additional 1.2nm bandpass filter is attached after the EDFA to suppress its ASE. To observe the high speed signal, a digital communications analyzer (DCA) is used to collect the data. Fiber polarization controllers are used to align the polarization of the pump and signal beams. Both the signal and the pump beams are aligned with the TE mode of the waveguide. The device under test is mounted on a thermo-electric cooler and kept at a temperature of 20°C.

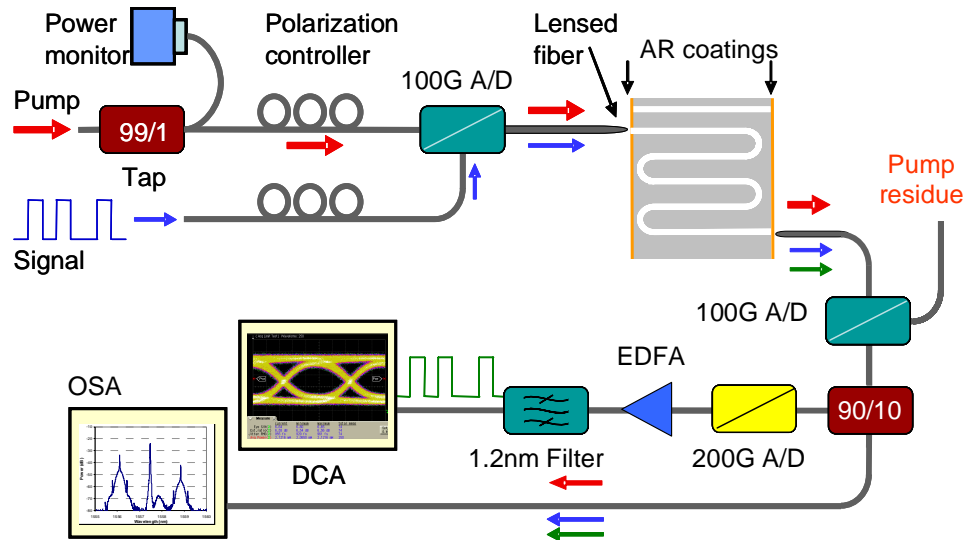


Fig. 1. Schematic of the experimental setup for 40 Gb/s wavelength conversion experiment

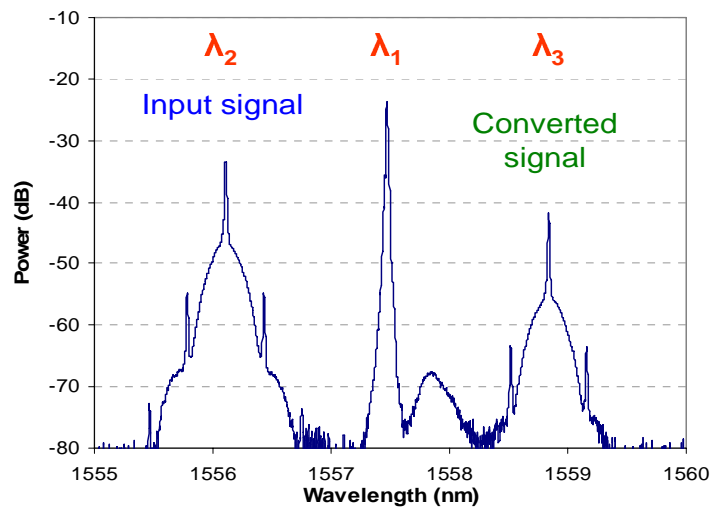


Fig. 2. Spectrum of the output beam from an 8-cm long waveguide. Coupled pump power is 450 mW, and the conversion efficiency in this example is -8.6 dB. Clear 40GHz sidebands can be seen both from the input and converted signal.

Figure 2 is a typical spectrum of the output beam from the silicon waveguide. In this example, the pump is at $\lambda_1=1557.48$ nm, and the input signal at $\lambda_2=1556.11$ nm. A new wavelength is generated at $\lambda_3=1558.85$ nm, which is exactly where the FWM process predicted, namely $1/\lambda_3=2/\lambda_1-1/\lambda_2$. For easy comparison with other published works, we follow the definition of wavelength conversion efficiency as the ratio between the peak levels of the converted signal at λ_3 and the original signal at λ_2 in Fig. 2. The conversion efficiency shown here is -8.6 dB for an 8-cm long waveguide with pump power of 450mW into the waveguide. We notice that both 40GHz sidebands are well converted to the new wavelength. The power ratio between the carrier and sidebands of ~22dB is maintained before and after the conversion. The

conversion bandwidth depends on the waveguide length and phase matching conditions [24, 25] and is estimated to be $\sim 7\text{nm}$ based on our previous measurements using a 4.8cm waveguide. [25]

The conversion efficiency is also measured as a function of the pump power for an 8 cm long waveguide at various bias voltages. As shown in Fig. 3, at low pump powers, slope efficiency is close to 2 as predicted by FWM theory [31], which is indicated with the dashed line in the plot. In cases of high pump powers, the nonlinear absorption starts to reduce the effective pump power and the slope efficiency drops to ~ 1.4 . By applying reverse bias voltage to the p-i-n diode in the waveguide, the two-photon absorption generated free carriers get swept out and the conversion efficiency significantly increases. In Fig. 3, at a pump power of 450 mW or intensity of 28 W/cm^2 inside the waveguide, a conversion efficiency of -8.6 dB can be reached with -25 V reverse bias. That is 2.9dB improvement compared to the open-circuit case and 1.7dB improvement compared to the short-circuit or 0V bias case.

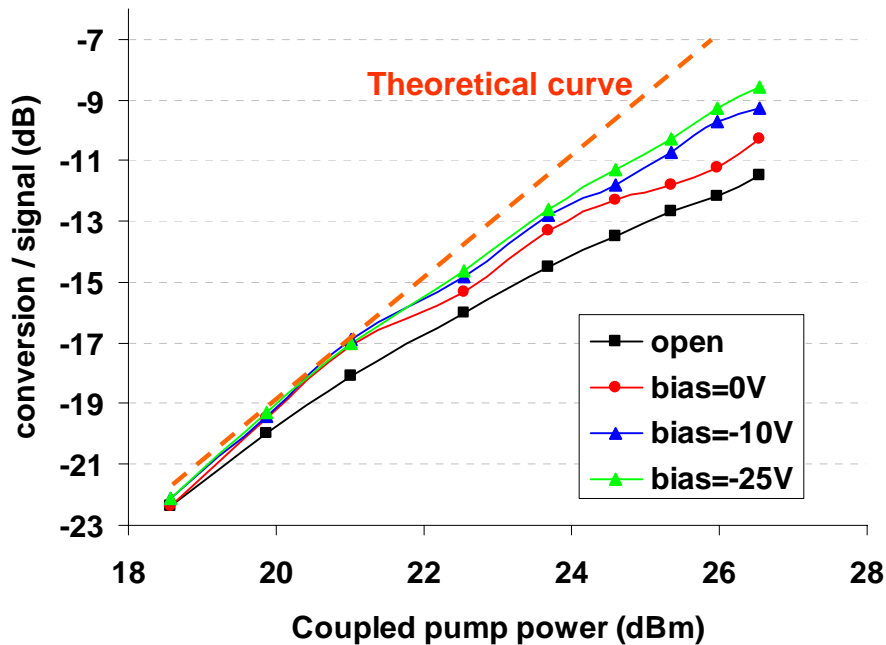


Fig. 3. Wavelength conversion efficiency as a function of pump power coupled into the waveguide for an 8 cm long double S-bend waveguide at different bias voltages. The dashed line indicates a theoretical FWM efficiency ignoring nonlinear losses.

To demonstrate the conversion of high-speed optical data, we modulate the input signal with a pseudo-random bit sequence at 40 Gb/s rate and measure the converted signal on the new wavelength. Since the pump power is held constant in our configuration, the conversion speed is practically not affected by the carrier decay time. Figure 4 shows the eye diagrams of the input and the converted 40 Gb/s optical data. The converted signal shows clear open eyes. The jitter is slightly increased, which may result from the pump noise and phase mismatch between different wavelengths.

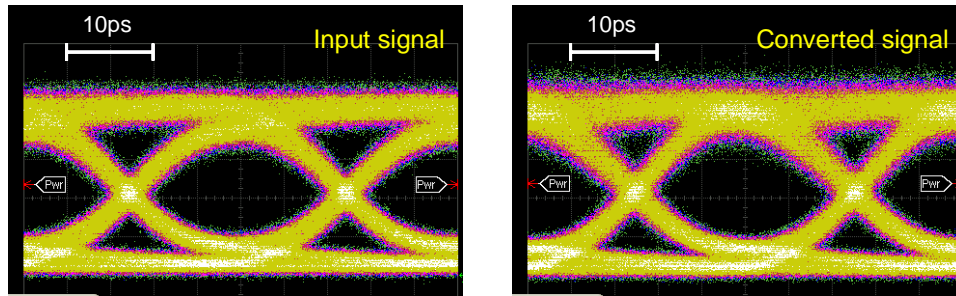


Fig. 4. Eye diagrams of the converted (right) signal in comparison with input (left) signal at 40Gb/s

4. Conclusion

To our knowledge, we have demonstrated, for the first time, wavelength conversion at 40 Gb/s data rate in silicon waveguides. Conversion efficiency as high as -8.6dB has been measured. By reverse biasing a p-i-n diode, we can reduce the carrier decay time and improve the conversion efficiency by ~3dB. While free carrier dynamics still is a limiting factor to the conversion efficiency, it does not affect the speed of the wavelength conversion at this data rate. By modifying waveguide dimensions and optimizing the p-i-n diode design, the carrier lifetime could be further reduced to achieve higher conversion efficiency. Using resonant structures such as ring resonators [23, 32], the required pump power can be reduced without sacrificing the signal bandwidth. By proper design of the waveguide dimensions to meet phase matching conditions [27, 33] higher conversion efficiency with broader conversion band width can be achieved.

Acknowledgments

The authors thank A. Liu, R. Jones, L. Liao, and O. Raday for technical discussions; N. Izhaky, D. Tran, K. Callegari, and H. Nguyen for assistance in device fabrication, sample preparation, and testing.